Stable Carbon Isotopes of Gaseous Alkanes as Genetic Indicators Inferred from Laboratory Pyrolysis Experiments of Various Marine Hydrocarbon Source Material from Southern China*

Wenhui Liu[1], Jie Wang[1], Tenger[1], Jianzhong Qin[1], and Lunju Zheng[1]

Search and Discovery Article #40945 (2012)
Posted June 11, 2012

*Adapted from extended abstract prepared in conjunction with poster presentation at AAPG Annual Convention and Exhibition, Long Beach, California, April 22-25, 2012, AAPG©2012

[1]Wuxi Institute of Petroleum Geology, SINOPEC, Wuxi 214151, China (wangjie.syky@sinopec.com)

Abstract

Using high pressure and geological conditions simulation vessels, hydrous pyrolysis experiments of kerogen, solid bitumen and liquid hydrocarbons from southern China were carried out in order to study the processes of gas generation and derive geochemical indicators of gas genesis in approximate geological conditions of pressure and temperature. The results indicate that gas generation productivity of different marine material decreased in the order of crude oil (light oil and condensate), dispersed soluble organic matter (solid bitumen and heavy oil), and kerogen. Under identical temperature-pressure regimes, pyrolysates derived from kerogen and dispersed soluble organic matter display drastically different geochemical characteristics. For example, the $\delta^{13}C_{CO2}$-$\delta^{13}C_1$ values of gaseous products from dispersed soluble organic matter are greater than 20‰, while those from kerogen are less than 20‰. The $\delta^{13}C_1$ values of pyrolysates from different marine hydrocarbon sources generally increase with pyrolysis temperature, but are always lower than that of the source precursors. The $\delta^{13}C$ values of ethane and propane in the pyrolysates also increase with increasing pyrolysis temperature, eventually approaching that of their sources, at peak hydrocarbon generation. At high-over mature stages, the $\delta^{13}C$ values of ethane and propane are often greater than that of their sources but close to those of coal gases, and thus become ineffective as gas genetic indicators.

Ln (C_2/C_3) can clearly distinguish gases derived from kerogen degradation and oil cracking and Ln (C_1/C_2) – ($\delta^{13}C_1$-$\delta^{13}C_2$) can be an effective indicator for distinguishing gases derived from oil- and dispersed-soluble organic matter cracking. Previous studies performed on different source organic matter lead to important understanding of gas geochemistry (Ma, 2008; Liu et al., 2006; Berner et al., 1996; Cramer et al., 2001). As the complete gas series derived from a given source from low to high-over maturity stage seldom exists in nature, the geochemistry and evolution process of natural gas from the same source remains a puzzle. Earlier studies focused on the simulation of gas generation from simple organic matter, with degrees of success (Behar et a1., 1992; Cramer, 2004; Wang et al., 2001; Wang et al., 2008; Tian et al., 2007), including the demonstration of key gas generation mechanisms and processes. These works have firmly laid the

foundation for establishing the kinetics model of gas generation, gas geochemistry systematics, and key indicators for discriminating gases from oil cracking and kerogen degradation. However, many problems remain unresolved and applying scopes of several distinguishing indicators were limited, particularly for oil-derived gases at high maturity. Moreover, there is a critical lack of demonstration on the variation of geochemical characteristics of natural gas derived from a single source but at different maturity stages.

Hydrous pyrolysis experiments can be used to study systematically the gas generation processes from organic matter, deriving important constraints for gas geochemistry and gas-source correlation. The theoretical basis for laboratory thermal simulation is that large organic molecules are gradually cracked to form small molecules in a manner similar to those in the subsurface geological regime. According to kinetic theory, temperature can be used to compensate the time, so the primary simulation experiment only took into account the effect of temperature on the hydrocarbon producing process. In order to simulate the geological reality, temperature, organic matter type, time, pressure, catalyst and rock matrix are among the key variables that have to be considered in simulation experiments. The experiments can be conducted in either open system (Cramer et al., 2001), semi-open system (Mi et al., 2007), or closed system (Xiao et al., 2007; Zhenget al., 2009). Different systems have different merits, depending on the specific aim and objectives of each study. Some geochemical indicators and templates for distinguishing gases from oil cracking and kerogen degradation were established from experiments involving sealed golden vessel (Behar et a1., 1992; Prinzhofer and Huc, 1995). This article focuses on simulation of gas generation from different types of marine organic matter, using high pressure vessels under various closed and semi-open systems. We report here the key geochemical characteristics and implications for gas generation from different types of organic matter in mid-high maturity stages.

Samples

Kerogens are commonly classified into three genetic types, but this classification cannot meet our needs for studying gas generation from different marine hydrocarbon sources other than kerogen. On the basis of genetic type, property and evolution of organic matter, hydrocarbon sources can be divided into soluble, insoluble and acid soluble organic matter. According to the host type, organic matter can also be divided into dispersed, enriched and chemically bound types. Coal and oil shale are highly enriched organic matter; both dispersed and enriched organic matter are found in so-called hydrocarbon source rocks. Secondary hydrocarbon sources include dispersed soluble organic matter within and outside of common source rocks, and enriched soluble organic matter (Dai, 2003; Cai et al., 2006), e.g. solid bitumen, heavy oil, migra-bitumen or other soluble organic matter remaining in hydrocarbon source rocks, reservoirs and carrier beds, which can reproduce and re-expel hydrocarbons (Qin et al., 2007; Zheng, et al., 2008). Dispersed and enriched soluble organic matter can undergo subsequent evolution or oxidation to form altered soluble organic matter, one of the most important secondary hydrocarbon sources. Moreover, diagenesis process of organic matter can form organic-inorganic complexes such as organic acid salts, an important chemical hydrocarbon source (Lei, et al., 2009). Different types of hydrocarbon sources coexist, reciprocally transform, and simultaneously or successively produce hydrocarbons in marine hydrocarbon source rocks, especially the state switching and the relaying of generating hydrocarbon process and contribution in marine hydrocarbon source rocks in southern China; it takes on the gas evolution characteristics of multi-source complex and multi-stage continuity.

In order to better understand the coexistence of various marine hydrocarbon sources, different types of marine hydrocarbon sources were subjected to pyrolysis in high pressure and geological condition simulation vessels. The basic geochemical data of the used samples are shown in Table 1.

Pyrolysis Experiments and Analytical Conditions

In order to study the effect of pore fluid pressure, space and high temperature liquid water on hydrocarbon generation processes and gaseous hydrocarbon geochemistry, pyrolysis experiments were conducted in a closed system, high pressure vessels and a semi-open geological conditions simulation vessel. High pressure vessel experiments were carried out with pressure ranging from atmosphere to 25 MPa and temperature from ambient to 600℃. The geological conditions simulation vessel experiments were conducted in approximate geological condition liquid pressure, confined pore space and the overlying lithostatic pressure.

In order to simulate gas generation from low maturity to high maturity stages, the pyrolysis temperatures used range from 200℃ to 550℃, with a heating rate at 1^{o}C/min and then staying at constant temperature for 48-96 h. Ten to 50% by weight of water bearing vapor was added to the high pressure vessel and saturate sample pore space and vessel space in the geological condition simulation vessel. Fluid pressure in the closed systems ranges from atmospheric pressure to 25 MPa (uncontrollable), while those in the semi-open systems vary from a few MPa to 150 MPa (controllable) to simulate hydrocarbon sources at different burial depth. The overlying lithostatic pressure is not imposed in the high pressure vessel, but added from tens to 200 MPa in the geological conditions simulation vessel. Rock chips were used in high pressure simulation, and original rock samples were used to preserve the original sample pore and structure in the geological conditions simulation. For experiments with crude oils, added rock matrix was pure limestone that had been extracted with chloroform and treated in high a temperature closed system.

Deionized water and the sample were added into the reaction vessel, which was sealed and pumped to vacuum. The pyrolysis experiments were conducted at different sets of temperature and pressure combinations to represent different geological settings. The pyrolysates were collected and weighted after the temperature inside the reaction vessel had dropped to 150℃. When the fluid pressure exceeded the given value, the products were collected and weighted in the geological conditions simulation. The compositions and carbon isotopes of gaseous products were analyzed and listed in Table 2.

Results and Discussion

Gas Composition and Characteristics

Gaseous products in the pyrolysates consist mainly of hydrocarbon gases, carbon dioxide, and hydrogen, with subordinate amounts of nitrogen and carbon monoxide. Gaseous hydrocarbon production from crude oil has the highest yields, increasing rapidly with increasing pyrolysis temperature above 400℃ and more modestly above 500℃ (Table 2 and Figure1). The gas yields from dispersed soluble organic matter come second, followed by those of kerogens. As a result, gas sources with higher soluble organic matter show higher gaseous

hydrocarbon yields at any given pyrolysis temperature. The hydrocarbon gas yield of a source rock generally correlates positively with increasing organic content, but negatively with thermal maturity. In general, hydrocarbon gas yields are higher in closed system pyrolysis than in semi-closed system, and the difference becomes much smaller under higher temperature regimes.

The pyrolysates consist mainly of methane, whose yields peaked at 500℃. The C_{2+} hydrocarbon gas yields are the highest at 400℃ or 500℃, depending on the source types, where better quality organic matter type tends to show higher temperature. Thermal cracking of higher molecular weight alkanes to form methane may be invoked to explain our observations. The contents and isotope compositions of carbon dioxide are different for kerogens and dispersed soluble organic matter (Figure 2). The $\delta^{13}C_{CO2}$-$\delta^{13}C_1$ values of gaseous products from dispersed soluble organic matter are greater than 20‰, while those of gaseous products from kerogens are lower than 20‰, indicating the isotope fractionation between carbon dioxide and methane derived from soluble organic matter is greater than those from kerogen.

Pyrolysis of Guangyuan bitumen and Canadian heavy oil shows increased $\delta^{13}C_{CO2}$ value with increasing carbon dioxide content in the pyrolysate, indicating a contribution from carbonate decomposition. In contrast, pyrolysates of other samples in this study generally show decreased $\delta^{13}C_{CO2}$ value with increasing carbon dioxide content, indicating a different mechanisms for CO_2 generation.

Stable Carbon Isotopes of Hydrocarbon Gases

In the early stage of thermal cracking, the $\delta^{13}C$ value of methane is relatively low, but higher values are observed in pyrolysates from crude oil and dispersed soluble organic matter, as a result of low temperature hydrocarbon cracking and polymerization (Xiong et al., 2004). With increasing thermal maturity, $\delta^{13}C$ value of methane increases but is lower than that of their hydrocarbon sources. The clear source control on hydrocarbon gas $\delta^{13}C$ value is illustrated in Figure 3. Because thermal maturity significantly affects methane isotopes, the use of $\delta^{13}C$ value of methane as a source indicator can only be done for samples with similar maturity levels.

With increasing maturity, $\delta^{13}C$ values of ethane and propane also increase (Figure 3). At peak hydrocarbon gas generation (450-500 ℃, Figure 1), these values approach their source values, and can thus be used as source indicators. It is worth noting that the simulation temperature at which the $\delta^{13}C$ values of heavy hydrocarbon gases approach their source values is lower in kerogen pyrolysis than in pyrolysis of dispersed soluble organic matter, indicating lower activation energy for kerogen degradation than that required for thermal cracking of crude oil and dispersed soluble organic matter. Thus, in a given petroleum system, $\delta^{13}C$ values of the heavy hydrocarbon gases derived from kerogen approach those of their sources earlier than those from crude oil and dispersed soluble organic matter. However, the gaseous products from kerogen have far lower yields than those from crude oil and soluble organic matter. The reason for relative lower stable carbon isotope values of methane from oil cracking lies in prior fractionation occurring during the transformation from kerogen to crude oil. As a result of methane generation from C_{2+} hydrocarbons with lower carbon isotope values than that of crude oil, lower carbon isotope values are expected for the methane products. Under the same temperature, that the carbon isotopic compositions of methane and ethane in the geological condition vessel simulation are lighter than that in the high pressure vessel simulation is caused by the isotope fractionation induced by the pressure in the geological condition vessel simulation.

Regardless of their source, kerogen, crude oil, or dispersed soluble organic matter, the $\delta^{13}C$ values of produced methane and ethane gradually increase with increasing thermal evolution (Figure 4). At a high maturity stage, the carbon isotopic values of ethane from manifold sources are greater than the boundary value (-28‰ or -29‰) distinguishing coal type gas from oil type gas at present (Xu, 1994; Wang et al., 2006). Moreover, at the high-over mature stage (being greater than 400-500℃, Ro＞1.5), the $\delta^{13}C$ values of ethane and propane are greater than that of their hydrocarbon sources (Figure 3 and Figure 4), thus the sources types of natural gases have to be judged by a combination of the heavy hydrocarbon carbon isotopes and other indicators.

Differentiation of Gases Derived from Source Rock Thermal Degradation and Thermal Cracking of Soluble Organic Matter

If we look at the composition of gaseous products from various hydrocarbon sources, the Ln (C_1/C_2) ranges of gaseous products are not significantly different between those from different types of kerogen and dispersed soluble organic matter and Ln (C_1/C_2) values show similar trends with increasing pyrolysis temperature. However, the Ln (C_1/C_2) ranges of oil cracked gases are smaller than that from dispersed soluble organic matter (Figure 5). This is likely related to long chain aliphatic carbon cracking in crude oil, whereas relative low saturated hydrocarbon content and relative high heavy component in dispersed soluble organic matter. The compositions of original organic matter have a significant control on the compositions of gaseous products, thus the relatively more homogeneous original organic matter would give rise to less heterogeneous gaseous hydrocarbon compositions.

The variation in the Ln (C_2/C_3) values for gaseous products shows significant differences between different types of kerogen and dispersed soluble organic matter (Figure 6). At low pyrolysis temperatures, the Ln (C_2/C_3) values for gaseous products of crude oil and dispersed soluble organic matter vary very little. At higher temperatures (450-550℃), however, the Ln (C_2/C_3) values of gaseous products increase rapidly, the contents of C_2 also increase steadily, but the contents of C_3 change in different directions, until the peak hydrocarbon generation is reached (Figure 1). With increasing simulation temperature, the Ln (C_2/C_3) values of gaseous products from different type of kerogen also increase.

Previous researchers conclude that the C_1/C_2 ranges of gaseous products from crude oil are relatively small, with great C_2/C_3 scopes, indicating that reaction rates of C_3 Cracking into C_1 and C_2 being relatively great cause the large ranges of C_3 contents, whereas the C_1/C_2 scopes of gaseous products from kerogen are relatively great with a small C_2/C_3 range, indicating that C_1 contents increase quickly with relatively stable increasing of C_2 and C_3 evoke the large ranges of C_1 contents (Zheng et al., 2009; Behar et a1., 1992; Wang et al., 2006). In the paper, prior to peak hydrocarbon generation, the Ln (C_2/C_3) ranges of gaseous products from crude oil (dispersed soluble organic matter) cracked gas and kerogen degraded gas are relatively small, with a large Ln (C_1/C_2) range. The Ln (C_1/C_2) values show larger variation for crude oil (dispersed soluble organic matter) cracked gases than that of kerogen degraded gas. The Ln (C_1/C_2) values of crude oil cracked gas vary between 0 and 2, but the Ln (C_1/C_2) values of kerogen degraded gases are mostly between 1 and 2. At peak generation to over-mature stage, the Ln (C_2/C_3) change of gaseous products has a significant difference between manifold kerogen and crude oil (dispersed soluble organic matter). Relative to Ln (C_1/C_2), Ln (C_2/C_3) changing scope of crude oil (dispersed soluble organic matter) cracked gas is obviously bigger than that of kerogen degradation gas. Moreover, with increasing thermal simulation temperature, the Ln (C_2/C_3) increasing rate of crude oil (dispersed soluble organic matter) cracked gas is obviously bigger than that of kerogen degraded gas, indicating that in the

map of Ln (C_1/C_2) and Ln (C_2/C_3), the linear gradient of crude oil cracked gas is bigger than that of kerogen degraded gas (Figure 7), which being inconformity with the former, and the deficiencies of the former traditional plate are reformed (Behar et al., 1992). The Ln (C_2/C_3) could serve as an effective indicator for distinguishing kerogen degradation gas from crude oil (soluble organic matter) cracked gas, particularly in peak generation to over-mature stage.

Previous studies often use Ln (C_2/C_3) and $\delta^{13}C_2$-$\delta^{13}C_3$ as an indicator to distinguish gases derived from kerogen degradation and oil cracking, e.g. in Angola, Kansas, and Tarim Basin (Zheng et al., 2009; Behar et al., 1992; Zhao et al., 2001; Wang et al., 2006; Xu, 1994). The correlation between Ln (C_2/C_3) and $\delta^{13}C_2$-$\delta^{13}C_3$ is not used for identifying the natural gas origin in the paper. It indicates that evident difference for crude oil and soluble organic matter exists in the diagram of Ln (C_1/C_2) and $\delta^{13}C_1$-$\delta^{13}C_2$ (Figure 8). The Ln (C_1/C_2) ranges and the $\delta^{13}C_1$-$\delta^{13}C_2$ differences for soluble organic matter cracked gas both vary greatly, but both vary little for oil cracked gas. Crude oils consist mainly of long chain aliphatic compound, their component being relatively simple in the article, and the ranges of C_1/C_2 ratios and the differences of $\delta^{13}C_1$-$\delta^{13}C_2$ from gas products both are small. But the components of dispersed soluble organic matter are complex, and the ranges of C_1/C_2 ratios and the differences of $\delta^{13}C_1$-$\delta^{13}C_2$ from gas products both are great, so the components of original matrix control the components and isotopes characteristics of gaseous products. In this article, we conclude that Ln (C_1/C_2) and $^{13}C_1$-$\delta^{13}C_2$ can be used as an effective indicator for distinguishing oil cracked gas from soluble organic matter cracked gas.

Conclusions

Results of pyrolysis experiments in both closed system and semi-open systems reveal similar trends in the gas yields, chemical and stable carbon isotope compositions of pyrolysates:

1) With increasing pyrolysis temperature, the yields of methane and heavy hydrocarbon gases gradually increase, and then decrease after the experiments reach a certain temperature. Peak methane yields occur at higher temperature than that of heavy hydrocarbon gases. The gas composition and yields are also strongly dependent on the hydrocarbon sources.

2) The stable carbon isotope values of gaseous hydrocarbons become positive with increasing pyrolysis temperature, but $\delta^{13}C$ values of methane are always lower than that of their sources. At peak hydrocarbon generation, the $\delta^{13}C$ values of ethane and propane approach to that of their sources, but become higher at high-over maturity stages and thus cannot be used to identify their source types.

3) The chemical and stable carbon compositions of hydrocarbon gases are mainly controlled by gas source type, thus hydrocarbon sources with lower carbon isotopic values tend to generate gases with lower carbon isotopic values.

4) Ln (C_2/C_3) can be considered as an good indicator for distinguishing gases derived from kerogen degradation and gases from crude oil and soluble organic matter thermal cracking. Based on results from our work, the cross plot of C_1/C_2 and $\delta^{13}C_1$-$\delta^{13}C_2$ appear to be effective as differentiators for gases from oil cracking and gases from soluble organic matter cracking.

References

Behar, F., M. Vandenbroucke, S.C. Teermann, P.G. Hatcher, C. Leblond, and O. Lerat, 1995, Experimental simulation of gas generation from coals and a marine kerogen: Chemical Geology, v. 126/3-4, p. 247-260.

Behar, F., S. Kressmann, L. Rudkiewicz, and M. Vandenbroucke, 1992, Experimental simulation in a confined system and kinetic modeling of kerogen and oil cracking: Organic Geochemistry, v. 19/1-3, p. 173-189.

Berner, U., and E. Falter, 1996, Empirical carbon isotope maturity relationships for gases from algal kerogens and terrigenous organic matter, based on dry, open system pyrolysis: Organic Geochemistry, v. 24/10-11, p. 947-955.

Cai, Y., Y. Zhu, and R. Huang, 2006, Geochemical behaviors and origin of reservoir bitumen in Puguang gas pool: Oil & Gas Geology, v. 27/3, p. 340-348.

Cramer, B., 2004, Methane generation from coal during open system pyrolysis investigated by isotope specific, Gaussian distributed reaction kinetics: Organic Geochemistry, v. 35/4, p. 379-392.

Cramer, B., E. Faber, P. Gerling, and B.M. Krooss, 2001, Reaction kinetics of stable carbon isotopes in natural gas-insights from dry, open system pyrolysis experiments: Energy & Fuel, v. 15, p. 517-532.

Dai, J., 2003, Pool-forming periods and gas sources of Weiyuan gas field: Petroleum Geology & Experiment, v. 25/5, p. 473-479.

Lei, T., Y. Xia, J. Zheng, Y. Wang, Q. Meng, and M. Jin, 2009, Ketones-an important product during hydrocarbon formation of organic acid salt: Journal Of Mineralogy And Petrology, v. 29/2, p. 84-87.

Liu, W., 2009, Research progress on manifold hydrocarbon source and its trace system in marine strata: Natural Gas Geoscience, v. 20/1, p. 1-7.

Liu, W., D. Zhang, B. Gao, J. Zheng, and X. Wang, 2005, Multiple origins of natural gas and their significance: Oil & Gas Geology, v. 26/4, p. 393-401.

Ma, Y., 2008, Geochemical characteristics and origin of natural gases from Puguang gas field on Eastern Sichuan Basin: Natural Gas Geoscience, v. 19/1, p. 1-9.

Mi, J., J. Dai, S. Zhang, and X. Li, 2007, Study on the gas generating ability of coal in different systems: Natural Gas Geoscience, v. 18/2, p. 245-249.

Prinzhofer, A.A., and A.Y. Huc, 1995, Genetic and post-genetic molecular and isotopic fractionations in natural gases: Chemical Geology, v. 126/2, p. 281-290.

Qin, J., X. Fu, and X. Liu, 2007, Solid Bitumens in the Marine Carbonate Reservoir of Gas Field in the Northeast Area of the Sichuan Basin: Acta Geologica Sinica, v. 81/8, p. 1065-1071.

Tian, H., X.M. Xiao, X.Q. Li, Z.Y. Xiao, J.G. Shen and D.H. Liu, 2007, Comparison of gas generation and carbon isotope fractionation of methane from marine kerogen- and crude oil-cracking gases: Geochimica, v. 36/1, p. 71-77.

Wang, H., and X. Zhou, 2001, Formation modes of typical marine origin gas pools in tarim basin: Acta Petrolei Sinica, v. 22/1, p. 14-18.

Wang, J., J. Chen, T. Wang, Z. Feng, T. Lin, X. Wang, and M. Li, 2006, Gas source rocks and gas genetic type in Shuangcheng-Taipingchuan area of Songliao Basin: Acta Petrolei Sinica, v. 27/3 p. 16-21.

Wang, T., A. Geng, Y. Xiong, Z. Liao, and X. Li, 2008, Kinetic simulation study on generation of gaseous hydrocarbons from the pyrolysis of marine crude oil and its asphaitene in Tarim Basin: Acta Petrolei Sinica, v. 29/2, p. 167-174.

Wang, Z., X. Fu, S. Lu, and J. Qu, 2001, An analogue experiment of gas generating by crude oil cracking, characters of products and its significance: Natural Gas Industry, v. 21/3, p. 12-15.

Xiao, Z., G. Hu, and Z. Li, 2007, Effect of pressure on hydrocarbon generation of source rock in close system: Natural Gas Geoscience, v. 18/2, p. 284-288.

Xiong, Y., H. Zhang, X. Geng, and A. Geng, 2004, Thermal cracking of n -octodecane and its geochemical significance: Chinese Science Bulletin, v. 49/S1, p. 79-83.

Xu, Y., 1994, The natural gas origin theory and application, Beijing: Science press, p. 97-106.

Zhao, M., F. Zeng, S.F. Qin, et al., 2001**,** Two pyrolytic gases found and proved in talimu basin**:** Natural Gas Industry, v. 21/1, p. 35-39.

Zheng, L., J. Qin, S. He, G. Li, and Z. Li, 2009, Preliminary study of formation porosity thermocompression simulation experiment of hydrocarbon generation and expulsion: Petroleum Geology & Experiment, v. 31/3, p. 296-304.

Zheng, L., J. Qin, Q. Zhang, and Z. Zhang, 2008, Gas Generation Potentiality of Various Marine Crude Oil and Bitumen in China: Acta Geologica Sinica, v. 821/3, p. 360-365.

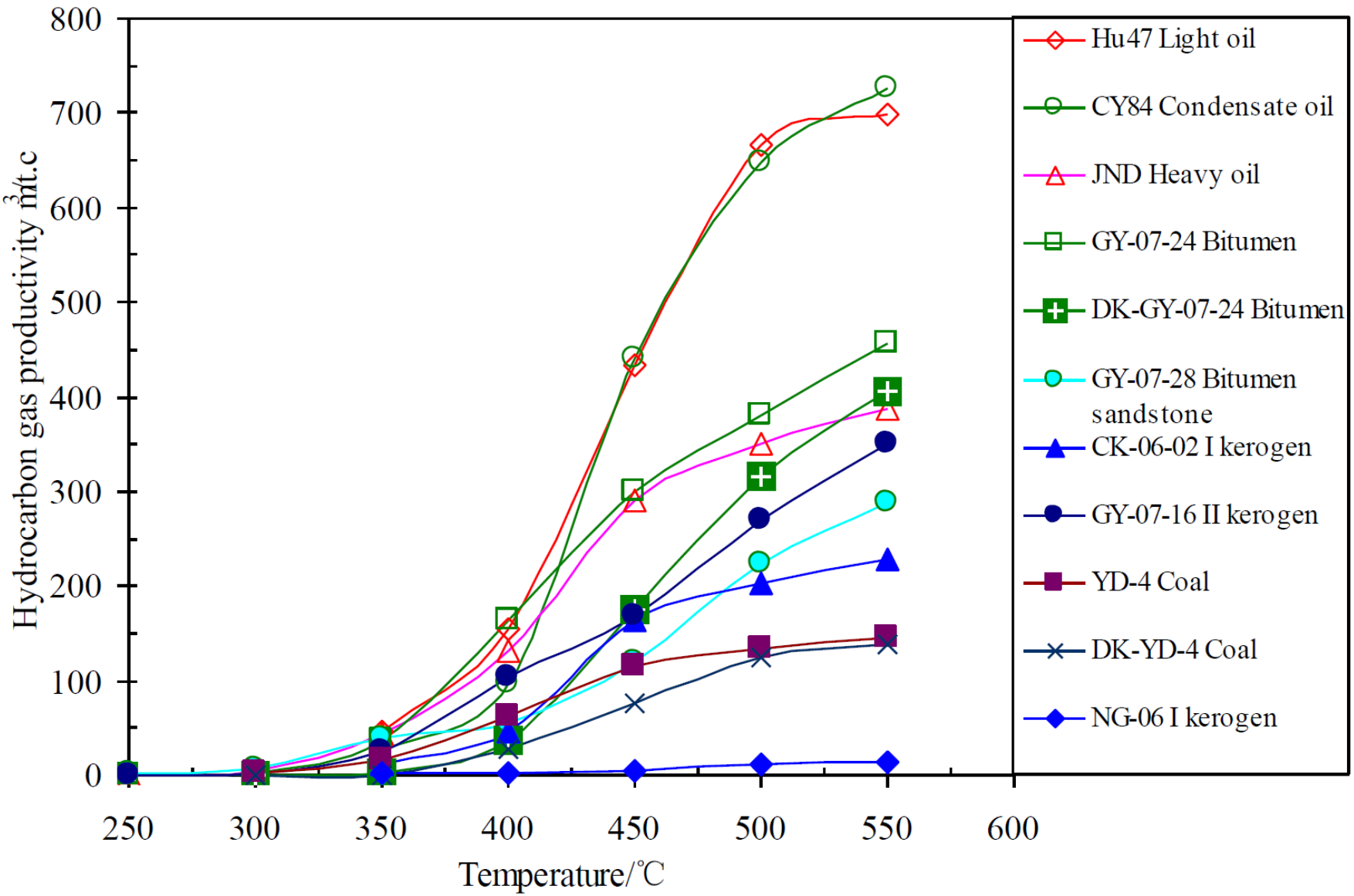

Figure 1. The productivity characteristics of hydrocarbon gas from simulation products in manifold sources.

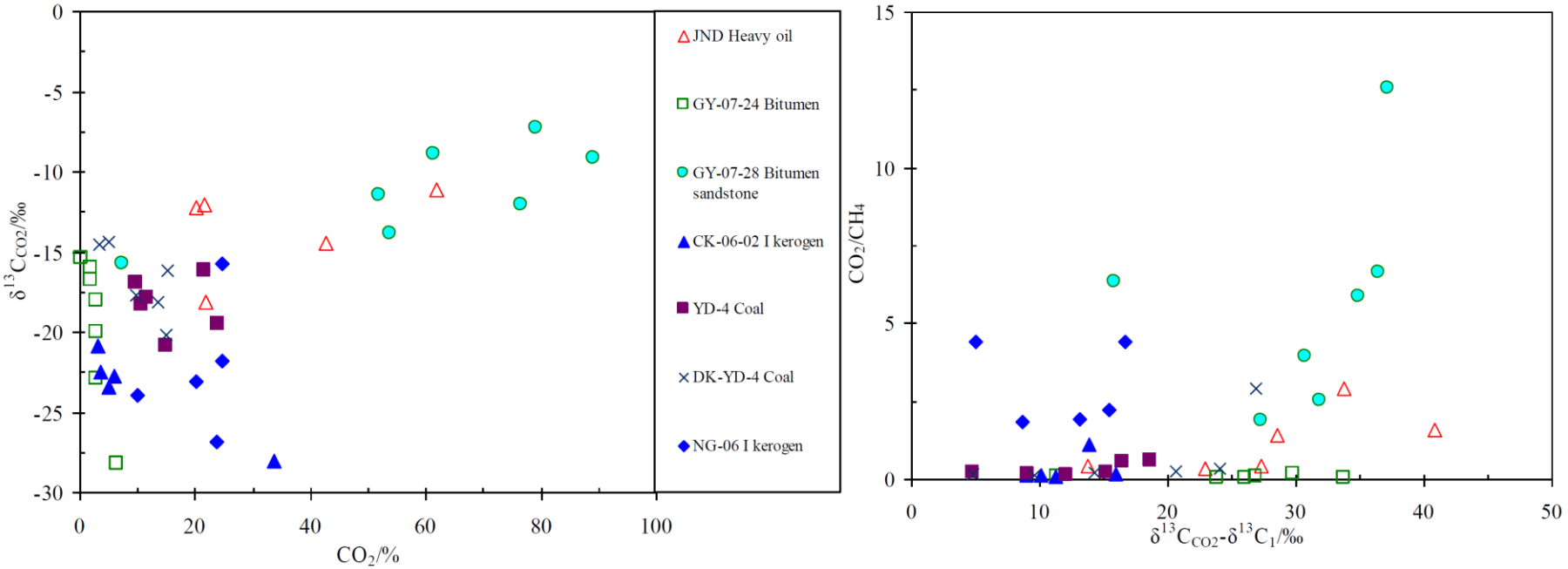

Figure 2. The correlation between CO_2 content and $\delta^{13}C_{CO2}$, CO_2/CH_4 and $\delta^{13}C_{CO2}$-$\delta^{13}C_1$ of gaseous products in manifold hydrocarbon sources.

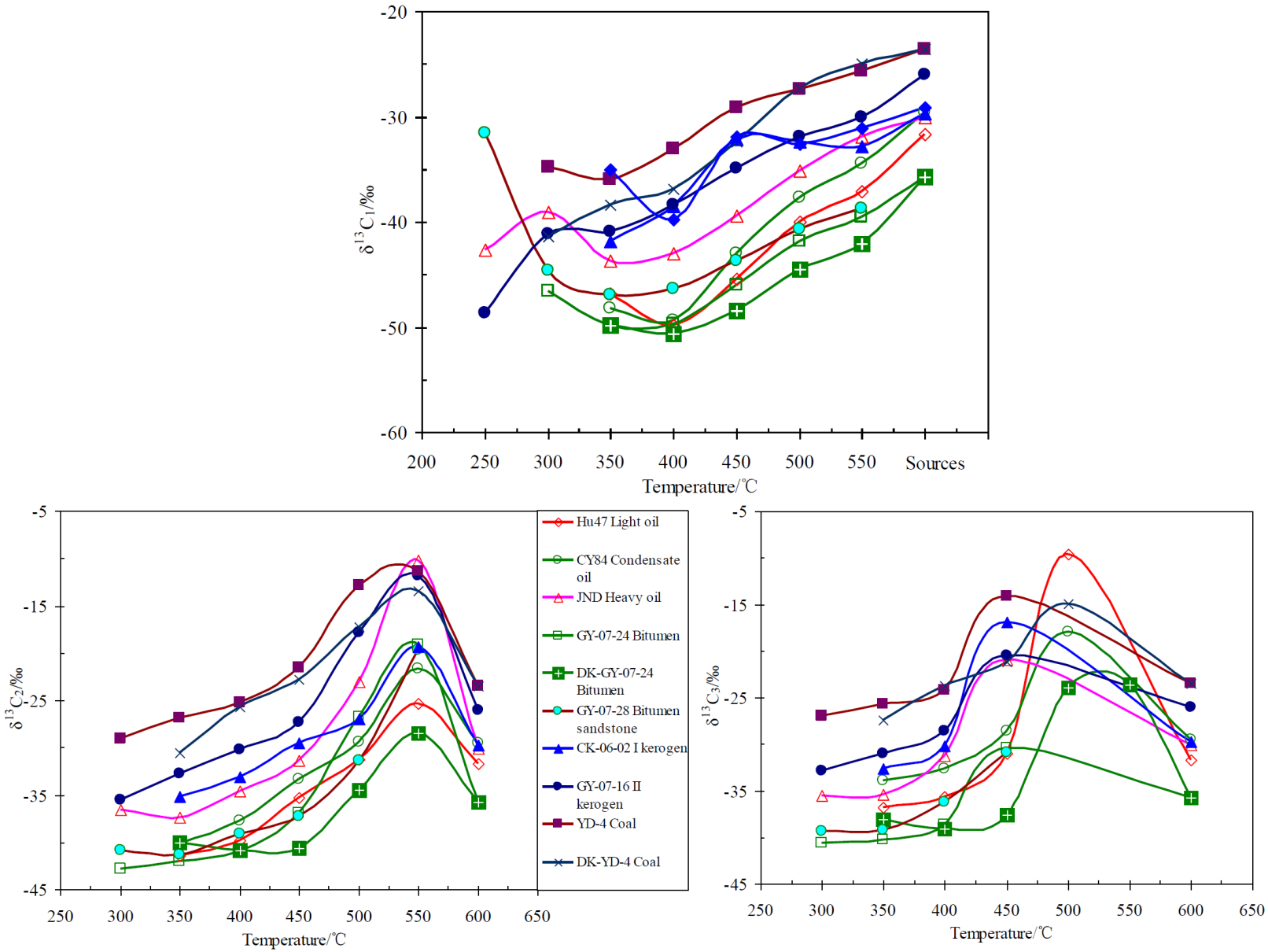

Figure 3. The varying characteristics of carbon isotopic compositions of hydrocarbon gaseous products in different types hydrocarbon sources.

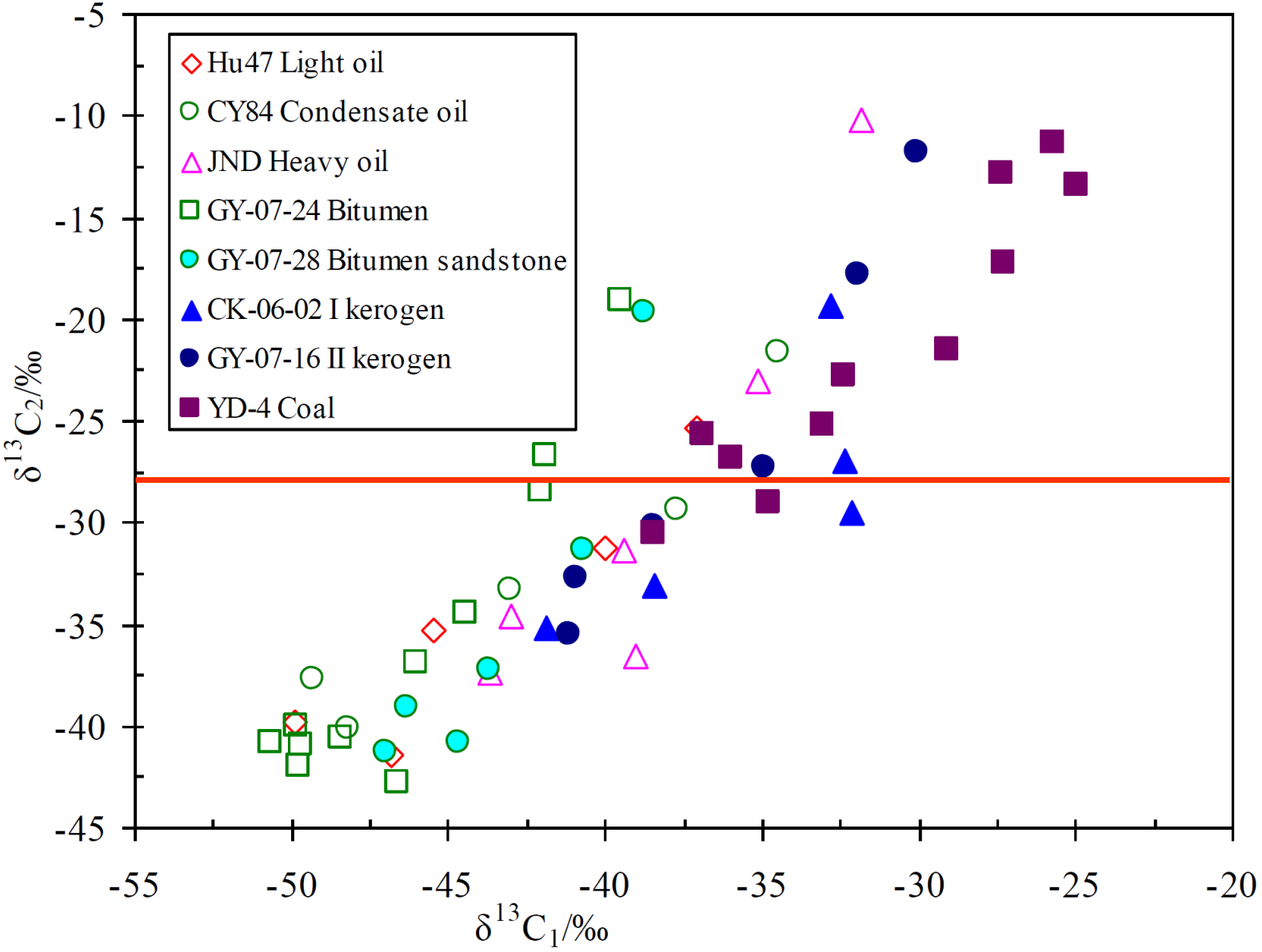

Figure 4. The carbon compositions of methane and ethane of gaseous products in manifold sources.

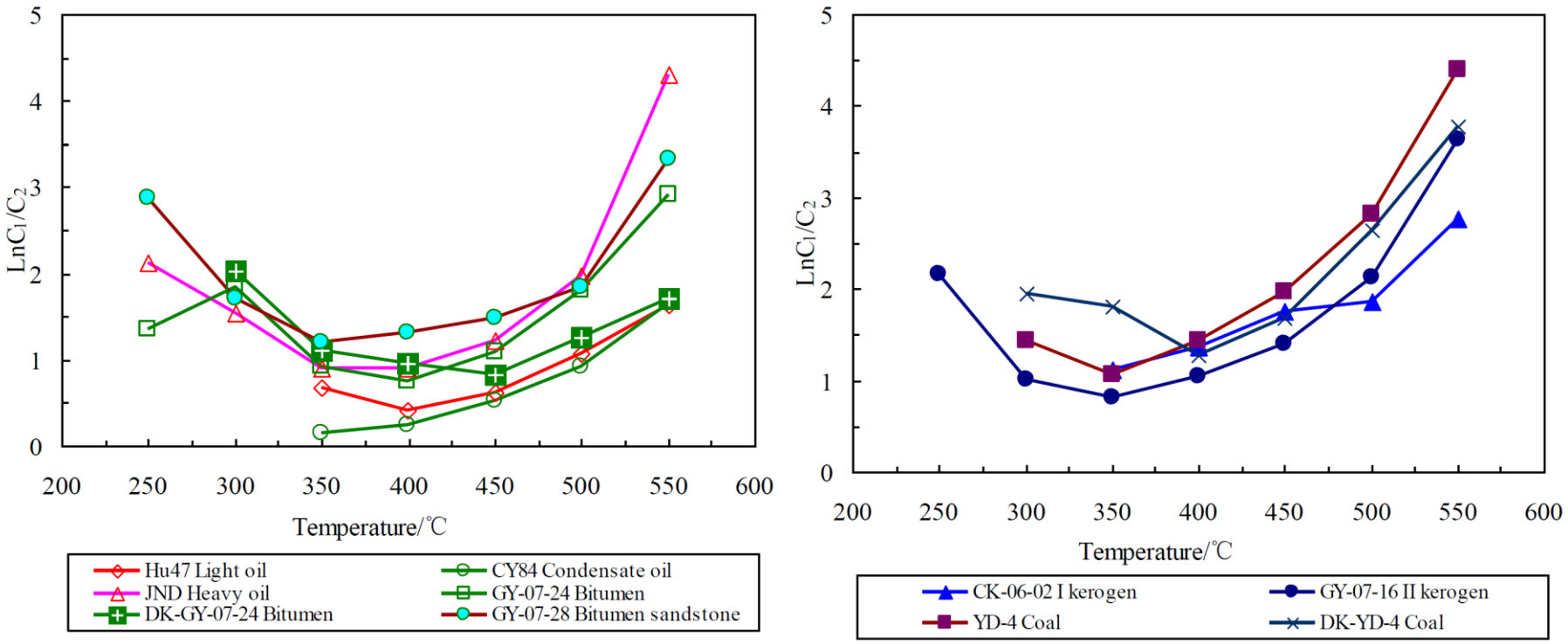

Figure 5. The varying rule of Ln (C_1/C_2) with temperature of gaseous products in different types sources.

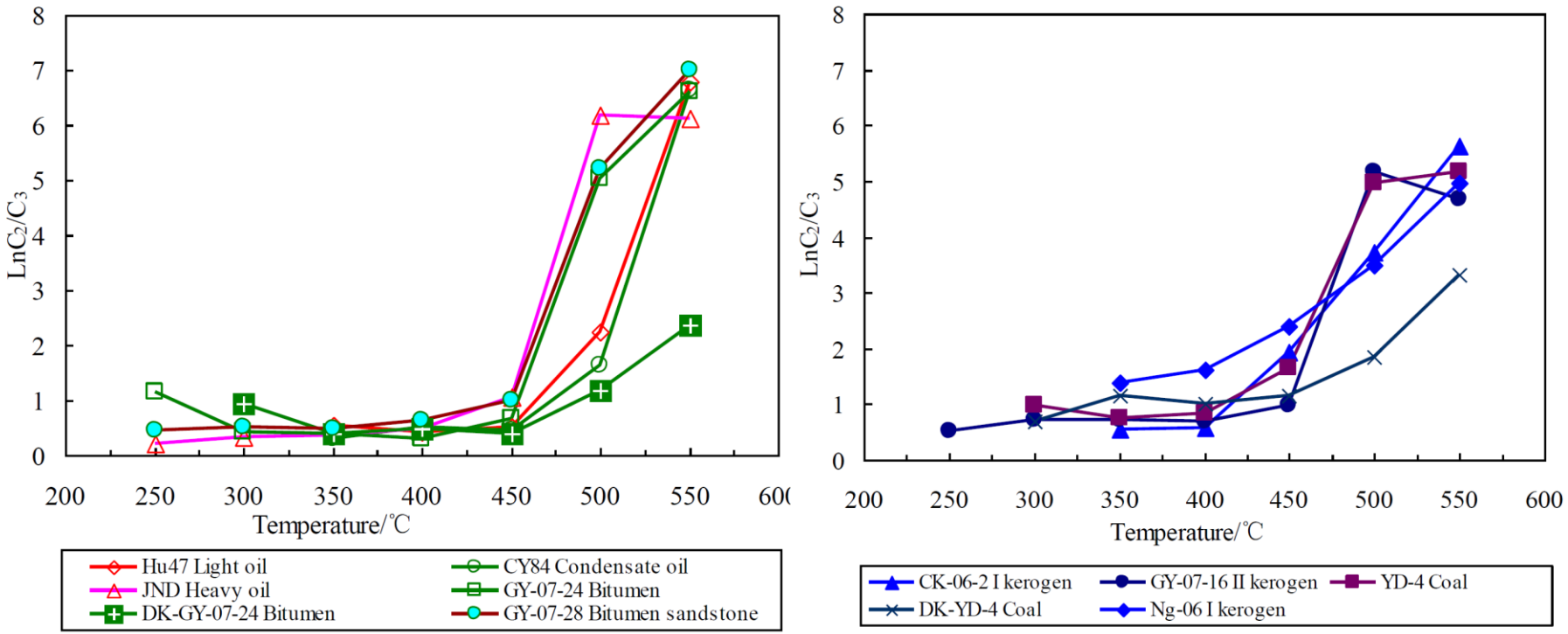

Figure 6. The varying rule of Ln (C_2/C_3) with temperature of gaseous products in different types.

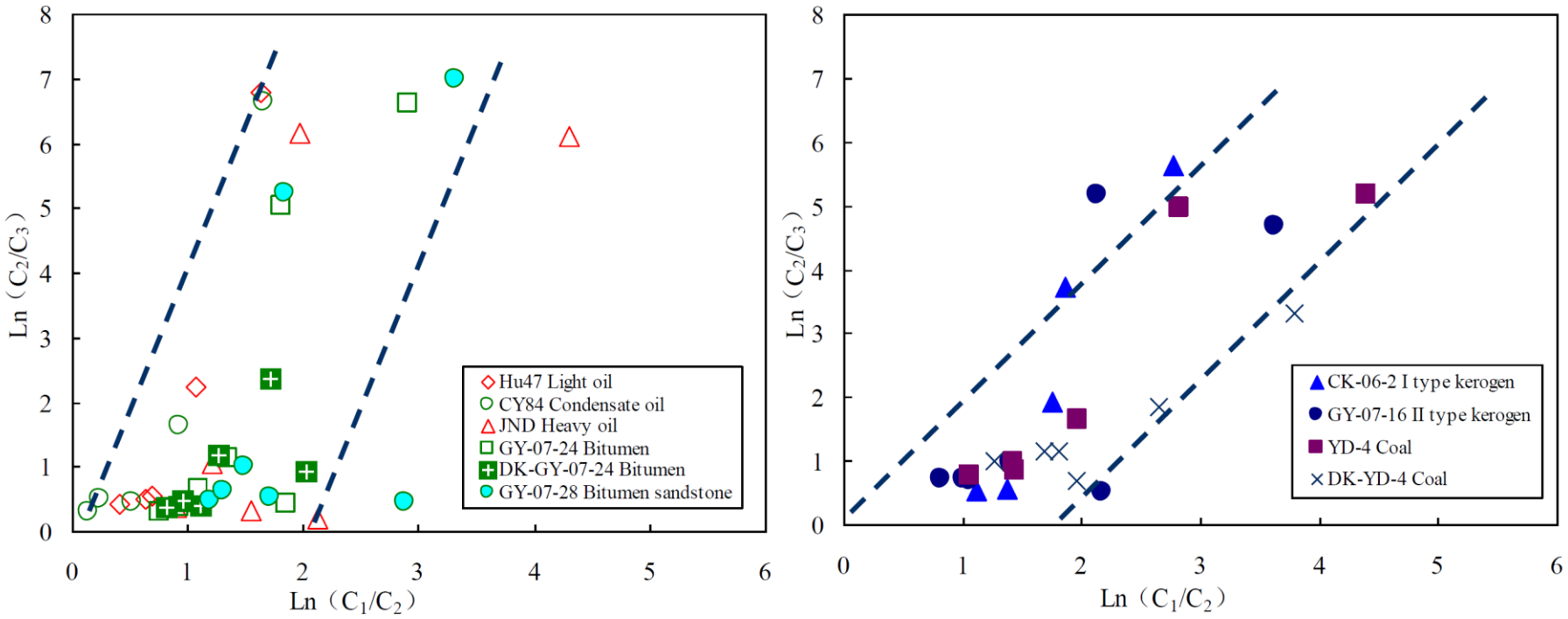

Figure 7. The correlation between Ln (C_1/C_2) and Ln (C_2/C_3) of gaseous products in different types sources.

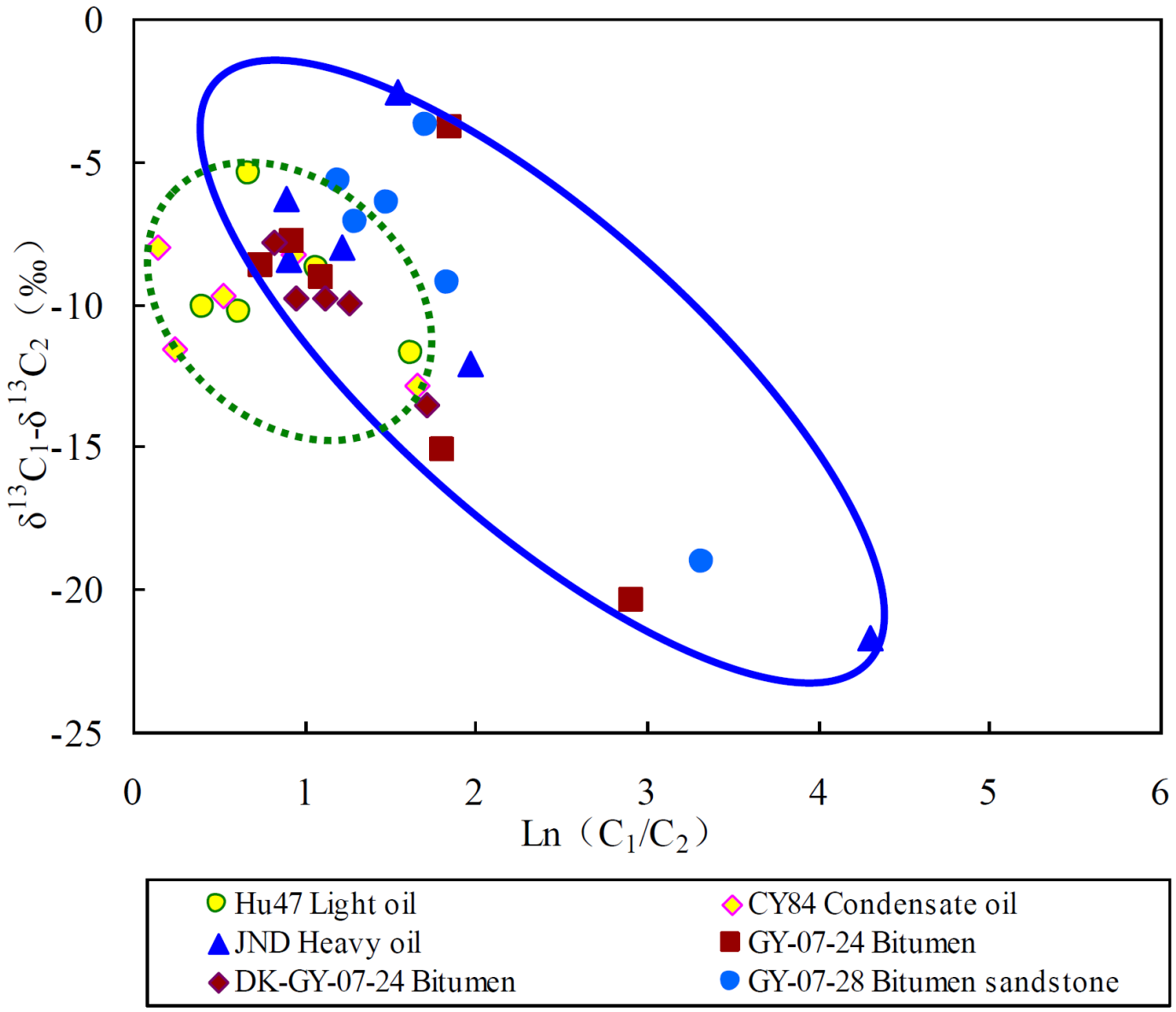

Figure 8. The characteristics of Ln (C_1/C_2) and $^{13}C_1$-$\delta^{13}C_2$ of hydrocarbon gas from different types sources.

Sample site	Sample No.	Sample type	stratum	TOC /%	Bitumen A /10^{-6}	$\delta^{13}C$/‰		HI mg/g	Ro/Rb %
						Kerogen	Bitumen A		
Dongyuezhai structure in Puguang	CY84	Condensate oil	T_1f				-29.6		1.03
Huzhuang structure in Kaili	Hu47	Light oil	S_1Wn				-31.7		-
West Canada Basin	CND	Heavy oil	D	10.59	147800		-30.0	673	-
Huoshi village in Qinchuan	GY-07-24	Solid bitumen	$\in$	78.67	229109		-35.8	510	0.5*
Hejiagou in Qinchuan	GY-07-28	Bitumen sandstone	$\in$	2.11	6531.3		-35.4	547	
Changjianggou in Guangyuan	GY-07-16	Black mudstone/II	P_2d	7.32	3027.1	-26.0	-27.1	365	0.7
Miaoba in Chengkou county	CK-06-02	Black shale/I	S_1lm	6.02	960.4	-29.8	-28.7		1.7*
Nangao in Danzhai county	NG-06	Black shale/I	$\in_1j$	4.25	10.04		-29.1		3.1*
Dapo coal mine in Yudong in Kaili	YD-4	Coal/III	P_2l	81.46	710.5	-23.5	-24.5	233	0.86

Table 1. The geochemical data of different types hydrocarbon sources in the simulation. Note: the column Ro/Rb marked with "*" indicating bitumen reflectance.

Table 2. page 1.

Sample No.	Hydrocarbon gas $m^3/t.c$	CO_2/%	C_1/%	C_2/%	C_3/%	$\delta^{13}C_{CO2}$ ‰	$\delta^{13}C_1$ ‰	$\delta^{13}C_2$ ‰	$\delta^{13}C_3$ ‰
Hu47-350	46.65	73.44*	10.07	5.08	2.90		-46.8	-41.4	-36.8
Hu47-400	153.44	57.28*	13.67	9.04	5.93		-49.9	-39.8	-35.7
Hu 47-450	432.89	34.43*	26.25	14.04	8.43		-45.5	-35.2	-31.0
Hu 47-500	665.33	40.66*	35.68	12.25	1.29		-40.0	-31.3	-9.6
Hu 47-550	697.82	50.87*	30.17	5.91	0.01		-37.1	-25.4	
CY84-350	26.46	81.44*	4.55	3.95	2.95	-2.6*	-48.2	-40.2	-34.0
CY84-400	97.39	59.79*	12.71	10.03	6.01	-0.6*	-49.3	-37.8	-32.6
CY84-450	439.86	35.91*	24.66	14.56	9.20	-0.8*	-43.0	-33.4	-28.6
CY84-500	648.34	46.68*	29.82	11.80	2.31	-1.7*	-37.7	-29.4	-17.9
CY84550	727.13	49.81*	29.25	5.59	0.01	-3.0*	-34.5	-21.6	
CND-250	0.16	61.87	2.95	0.35	0.29	-11.2	-42.7	-34.1	-32.9
CND-300	4.82	6.35	2.17	0.46	0.33	-5.2	-39.0	-36.5	-35.6
CND-350	43.87	32.23	20.46	8.35	5.78	-2.8	-43.7	-37.4	-35.4
CND-400	132.54	42.56	29.80	12.10	7.50	-14.5	-43.0	-34.5	-31.2
CND-450	291.36	21.58	48.06	14.26	4.92	-12.1	-39.4	-31.4	-20.9
CND-500	350.59	20.16	59.47	8.26	0.02	-12.2	-35.1	-23.0	
CND-550	386.42	21.90	51.91	0.70	0.00	-18.1	-31.9	-10.2	
GY-07-28-250	2.15	7.41	1.17	0.07	0.04	-15.7	-31.6	-39.2	-37.7
GY-07-28-300	7.08	53.74	13.57	2.45	1.45	-13.9	-44.6	-40.9	-39.4
GY-07-28-350	39.56	76.44	13.01	3.91	2.44	-12.1	-47.0	-41.3	-39.2
GY-07-28-400	55.66	89.11	7.08	1.92	1.02	-9.2	-46.3	-39.2	-36.2
GY-07-28-450	118.96	79.24	11.92	2.69	0.99	-7.2	-43.7	-37.2	-30.9
GY-07-28-500	223.88	61.29	24.2	3.85	0.02	-8.9	-40.7	-31.4	

Table 2. page 2.

			0						
GY-07-28-550	289.24	51.81	27.37	0.99	0.00	-11.4	-38.7	-19.6	
GY-07-24-250	0.31	0.29	0.86	0.22	0.07	-15.4	-45.3	-38.1	-34.3
GY-07-24-300	1.36	1.86	11.87	1.86	1.23	-16.8	-46.6	-42.8	-40.6
GY-07-24-350	36.36	2.76	27.21	10.77	7.34	-22.9	-49.8	-41.9	-40.2
GY-07-24-400	162.77	1.95	37.58	17.66	12.94	-16.0	-49.7	-41.0	-38.6
GY-07-24-450	299.70	2.88	54.38	18.13	9.41	-20.0	-46.0	-36.9	-30.4
GY-07-24-500	379.80	2.90	72.92	11.98	0.08	-18.0	-41.9	-26.7	
GY-07-24-550	456.35	6.45	63.19	3.43	0.00	-28.2	-39.5	-19.1	
DK-GY-07-24-300	0.29	17.6*	0.44	0.06	0.02	-3.6*	-44.8	-38.0	-34.0
DK-GY-07-24-350	1.94	43.8*	1.22	0.40	0.27	0.4*	-49.9	-40.1	-38.1
DK-GY-07-24-400	35.98	58.2*	17.61	6.79	4.20	-0.3*	-50.6	-40.8	-39.2
DK-GY-07-24-450	176.07	37.2*	30.88	13.63	9.25	-0.5*	-48.4	-40.6	-37.6
DK-GY-07-24-500	315.77	24.8*	53.40	15.07	4.62	-2.7*	-44.5	-34.5	-23.9
DK-GY-07-24-550	406.35	27.8*	58.10	10.42	0.99	-1.1*	-42.0	-28.5	-23.6
GY-07-16-250	0.18	30.43	2.30	0.26	0.16		-48.7	-37.4	-35.1
GY-07-16-300	2.13	67.48	10.60	3.88	1.87		-41.1	-35.6	-32.9
GY-07-16-350	26.38	32.75	23.77	10.59	5.17		-40.9	-32.7	-31.0
GY-07-16-400	104.23	34.67	30.13	10.50	5.24		-38.4	-30.3	-28.6
GY-07-16-450	168.30	43.24	37.19	9.24	3.45		-34.9	-27.3	-20.5
GY-07-16-500	269.12	46.95	40.68	4.84	0.03		-31.9	-17.9	
GY-07-16-550	350.68	49.96	36.82	0.98	0.01		-30.0	-11.8	
CK-06-02-350	12.20	33.57	30.01	9.82	5.67	-28.1	-41.9	-35.2	-32.7

Table 2. page 3.

CK-06-02-400	46.77	3.64	20.41	5.20	2.92	-22.5	-38.5	-33.1	-30.2
CK-06-02-450	163.02	3.14	33.66	5.84	0.84	-20.9	-32.1	-29.5	-16.9
CK-06-02-500	202.41	5.07	40.42	6.27	0.15	-23.5	-32.4	-27.0	-8.4
CK-06-02-550	228.84	6.02	49.54	3.12	0.01	-22.7	-32.9	-19.3	
YD-4-300	1.48	21.5	36.29	8.67	3.23	-16.1	-34.8	-29.0	-27.0
YD-4-350	16.17	23.8	42.71	14.85	6.95	-19.5	-36.0	-26.9	-25.7
YD-4-400	62.15	11.7	54.49	13.01	5.56	-17.9	-33.0	-25.2	-24.1
YD-4-450	114.69	9.8	69.35	9.72	1.88	-17.0	-29.1	-21.5	-14.2
YD-4-500	133.12	10.7	67.49	4.03	0.03	-18.3	-27.4	-12.8	
YD-4-550	144.39	14.9	67.77	0.84	0.00	-20.9	-25.7	-11.4	
DK-YD-4-300	0.02	3.3	1.14	0.16	0.08	-14.5	-41.3	-33.0	-27.7
DK-YD-4-350	0.24	5.0	15.16	2.48	0.78	-14.3	-38.4	-30.6	-27.5
DK-YD-4-400	26.53	15.1	58.09	16.34	5.96	-16.2	-36.8	-25.7	-23.7
DK-YD-4-450	75.18	13.6	68.12	12.74	4.01	-18.2	-32.4	-22.8	-21.2
DK-YD-4-500	125.32	9.8	82.52	5.84	0.92	-17.7	-27.3	-17.2	-15.0
DK-YD-4-550	138.47	14.9	81.75	1.86	0.07	-20.2	-24.9	-13.4	
NG-06-350	2.85	24.6	12.78	0.26	0.06	-21.8	-35.0	-40.4	-37.3
NG-06-400	2.58	20.1	4.54	0.12	0.02	-23.1	-39.8	-32.5	-27.6
NG-06-450	5.00	23.7	5.39	0.11	0.01	-26.8	-31.9	-31.2	-25.4
NG-06-500	10.83	10.0	5.48	0.39	0.01	-24.0	-32.6	-30.0	-18.9
NG-06-550	12.87	24.6	10.98	0.13	0.00	-15.7	-31.1	-22.0	

Table 2. The geochemistry of simulated gas from manifold hydrocarbon sources. Note: the last figure of the sample number is the simulation temperature. So called DK of the sample number represents the artificially geological condition simulation. "*" indicates the limestone added into the simulation sample.